DOI: 10.1002/chem.200500789

A Versatile Bis-Porphyrin Tweezer Host for the Assembly of Noncovalent Photoactive Architectures: A Photophysical Characterization of the Tweezers and Their Association with Porphyrins and Other Guests

Lucia Flamigni,*[a] Anna Maria Talarico,[a] Barbara Ventura,[a] Regis Rein,[b] and Nathalie Solladié*[b]

Abstract: A bis(Zn^{II}–porphyrin) tweezer host with anthracene components as apex and side-arms has been synthesized. Mono- (pyridine) and bidentate (4,4′-bipyridine) guests were used as models for single and double axial coordination inside the cavity, respectively. A series of dipyridylporphyrin guests with different substitution patterns and excited-state energy levels have association constants with the tweezers that are of the order of $10^6\,M^{-1}$, which is indicative of complexation with the inside of the cavity. This complexation can only occur upon an important distortion of the cavity that opens the bite by about 30%. This characteristic, in conjunction with their ability to reduce the bite distance by rotation around single bonds, makes these porphyrin tweezers amongst the most versatile so far reported, with tuning of the bite distance in the range of approximately 5–20 Å. Energy transfer to the free-base guest within the triporphyrin complex is nearly quantitative (95–98%) and the rates of transfer are consistent with a Förster mechanism that is characterized by a reduced orientation factor.

Keywords: energy transfer · luminescence · photochemistry · porphyrinoids · self-assembly · supramolecular chemistry

Introduction

The elaboration of noncovalent multiporphyrin assemblies represents an important challenge in the mimicry of bacterial photosynthesis[1] and the design of functional molecular materials.[2] Axial coordination to the central metal ions of porphyrins by suitable ligands is an effective and widespread strategy for the assembly of noncovalently bound, multicomponent systems. Zn^{II} derivatives[3–6] have been extensively used for this purpose, but examples based on Ru^{II},[7] Co^{II},[8] Rh^{III},[9] Sn^{IV},[10] P^{V},[11] and Al^{III}[12] porphyrins can also be found in the literature.

Pyridines with Zn^{II} porphyrins have rather weak association constants, of the order of 10^3–$10^4\,M^{-1}$ depending on their pK_a values and the steric hindrance at the nitrogen atom, and multiple recognition sites are required in order to obtain the high association constants that would allow these assemblies to be observed as the major molecular entity in solutions at spectroscopic concentrations.[6] Several bis(zinc–porphyrin) structures with a tweezer-like structure have been designed so far in order to effectively complex bidentate guests. Tweezers with chiral structures form a special class of these compounds and find applications in enantiomeric discrimination and in the determination of the absolute configuration of optically active guests.[13] Our interest lies in the design and study of photoactive multicomponent systems and we have been intrigued, as have other groups, by the possibility of using bis-porphyrin tweezers in solutions as hosts for convenient photo- or electroactive guests in order to assemble molecular structures with some degree of complexity that are able to undergo photoinduced energy or electron transfer.[14]

We herein report the photophysical properties of bis(zinc–porphyrin) tweezers with a skeleton consisting of anthracene chromophores connected by ethynyl bonds, **1** in Scheme 1, and examine its complexation properties with

[a] Dr. L. Flamigni, Dr. A. M. Talarico, Dr. B. Ventura
Istituto per la Sintesi Organica e Fotoreattivita' (ISOF), CNR
Via P. Gobetti 101, 40129 Bologna (Italy)
Fax: (+39) 051-639-9844
E-mail: flamigni@isof.cnr.it

[b] R. Rein, Dr. N. Solladié
Groupe de Synthèse de Systèmes Porphyriniques (G2SP)
Laboratoire de Chimie de Coordination du CNRS (UPR 8241)
205 route de Narbonne, 31077 Toulouse Cedex 4 (France)
Fax: (+33) 561-553-003
E-mail: solladie@lcc-toulouse.fr

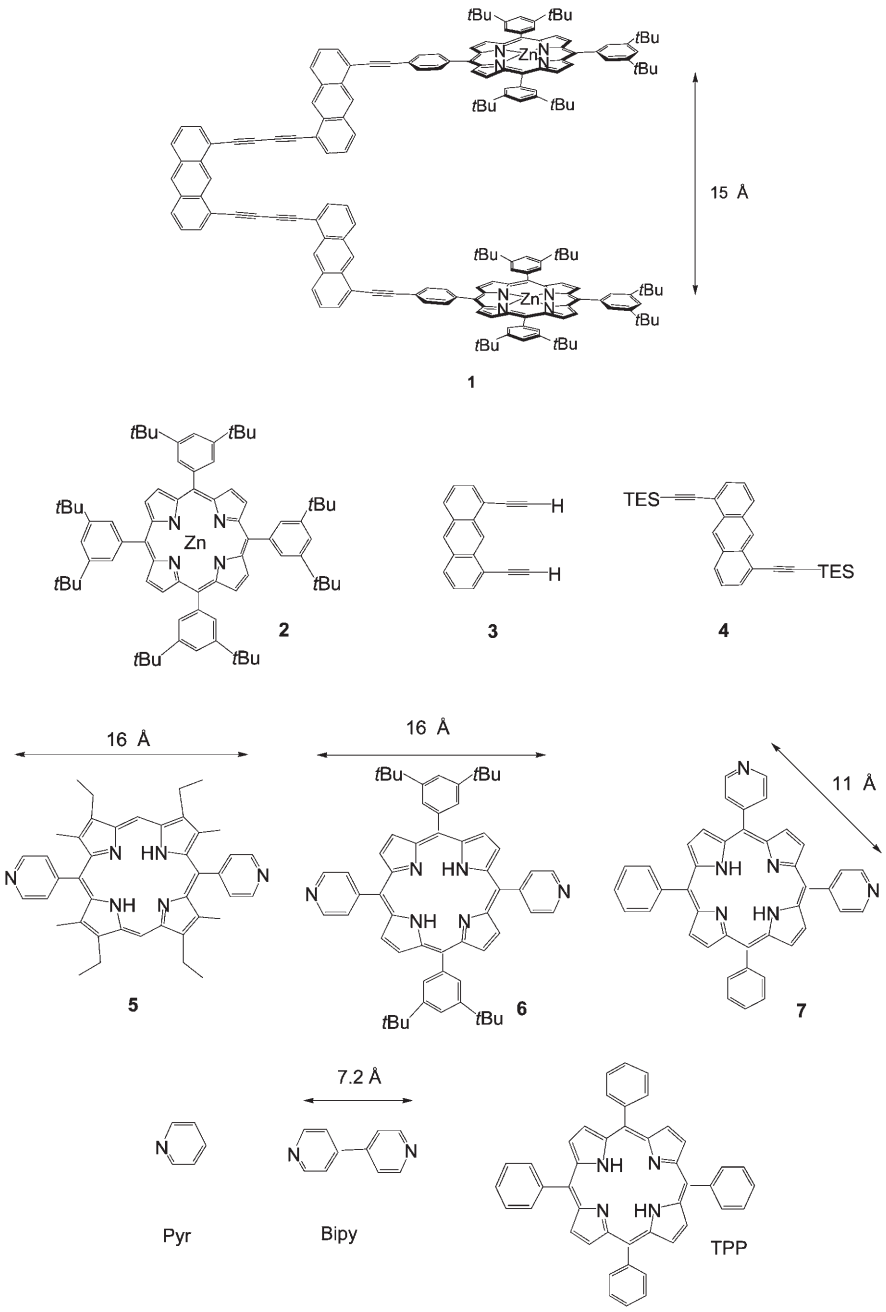

Scheme 1. Bis-porphyrin tweezers (**1**), component models (**2**–**4**), free-base porphyrin guests (**5**–**7**) and other guests described in this work.

photochemically innocent guests like pyridine (Pyr) and bipyridine (Bipy). Bis(zinc–porphyrin) **1** has a cavity defined by two nearly parallel zinc–porphyrins with a bite (Zn–Zn distance) at the maximum extension of approximately 15 Å, and it has been shown that through rotation around a single bond, the cavity can adjust to a smaller size with the two porphyrin planes close and cofacial (distance ca. 5 Å) and thereby efficiently complex small bidentate guests such as DABCO.[5] We have selected as potential guests a series of dipyridylporphyrins with different inter-pyridyl nitrogen (N–N) distances (Scheme 1). Porphyrins **5** and **6** have N–N distances of approximately 16 Å, whereas **7** has an N–N distance of about 11 Å. Taking into consideration the fact that the Zn–N bond length is about 2 Å, one can anticipate for **7** nearly perfect size-matching, whereas the fitting of **5** and **6** within the cavity would require some distortion of the tweezers' structure. We herein show that complexation of all porphyrins takes place with association constants typical of in-cavity complexation, indicating that these tweezers have a remarkably good degree of flexibility.

Finally we characterize and discuss the photoinduced processes that occur within the complexes formed by the bis-porphyrin tweezers and the free-base porphyrin guests **5**, **6**, and **7**, which are characterized by different excited-state energy levels.

Results and Discussion

Synthesis: The synthesis of dimer **1**, described in Scheme 2, relies upon the cross-coupling of two porphyrin–anthracene conjugates **11** to a central 1,8-bis(bromoethynyl)anthracene (**12**).[5] Compound **12** was obtained by bromination of 1,8-diethynylanthracene (**3**)[4] with *N*-bromosuccinimide and silver nitrate in acetone. The dissymmetrical 1-ethynyl-5-triethylsilylethynylanthracene (**8**) was prepared from the commercially available 1,5-dichloroanthraquinone. Statistical deprotection of one of the triethylsilyl protecting groups of 1,5-bis(triethylsilylethynyl)anthracene (**4**)[15] in a 85:15 mixture of THF/MeOH in the presence of potassium carbonate gave **8** in 43% yield, together with 16% of the fully deprotected compound and 33% of unreacted starting material. A Sonogashira coupling reaction was, at that stage, carried out between the free acetylene of **8** and the iodoporphyrin **9**[16] in degassed NEt_3 in the presence of $[Pd(PPh_3)_2Cl_2]$ and CuI. Compound **11** was obtained by subsequent deprotection of the triethylsilyl group in a 50:50 mixture of THF/MeOH in the presence of potassium carbonate. The desired tweezers **1**

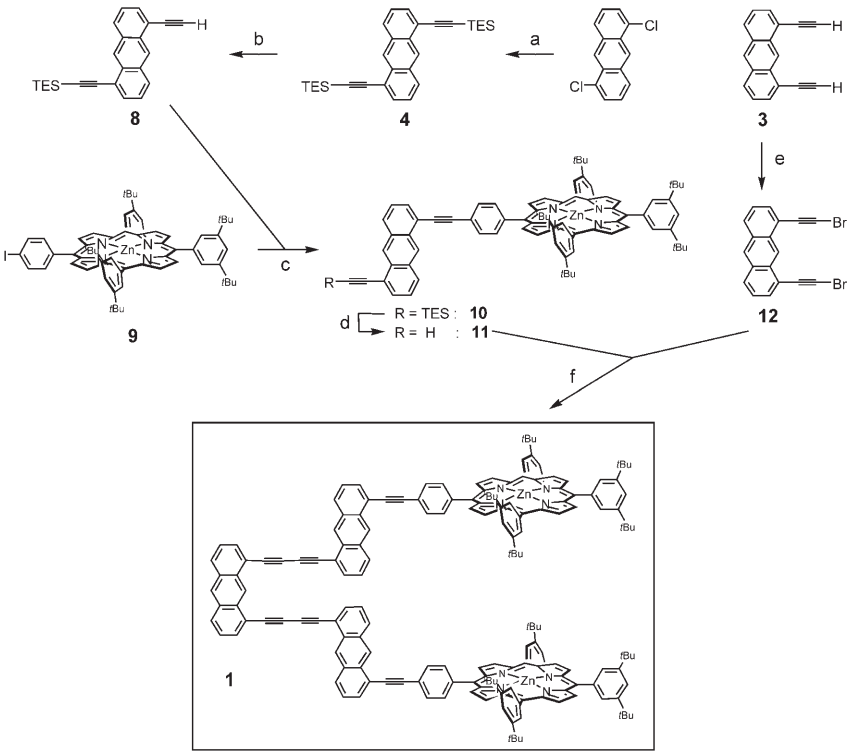

Scheme 2. Reagents and conditions: a) TESCCMgBr, PPh_3, $Ni(acac)_2$, THF, reflux, 25%; b) K_2CO_3, THF/CH_3OH 85:15, RT, 6 h 30 min, 43%; c) $[Pd(PPh_3)_2Cl_2]$, CuI, NEt_3, RT, 24 h, 58%; d) K_2CO_3, THF/CH_3OH 50:50, RT, 6 h, 87%; e) NBS (2.4 equiv), $AgNO_3$ (0.12 equiv), acetone, RT, 4 h, 87%; f) $[Pd_2(dba)_3]$ (0.02 equiv), CuI (0.025 equiv), LiI (0.2 equiv), PMP (2.8 equiv), DMSO, RT, 3 days, 33%.

were finally obtained by coupling two porphyrinic arms (**11**) to the central 1,8-bis(bromoethynyl)anthracene linker (**12**). Great difficulties were encountered in this step due to the formation of a homocoupling product. The heterocoupling conditions developed by Cai and Vasella gave the best results for the present purpose.[17] Two equivalents of **11** were allowed to react with one equivalent of **12** in degassed DMSO in the presence of $[Pd_2(dba)_3]$ (dba = dibenzylideneacetone), LiI, CuI, and 1,2,2,6,6-pentamethylpiperidine. After tedious preparative chromatography on Al_2O_3, the desired bis-porphyrin tweezers **1** were finally isolated in 33% yield.

The bis-porphyrin tweezers 1: Scheme 1 shows the various components, **2**–**4**, of the bis-porphyrin tweezers **1**. In a first approximation the tweezers can roughly be considered to consist of the following constituents: two units of **2** connected to two units **4** which in turn are linked to a common unit **3**. The absorption and emission spectra of units **3** and **4** in toluene at room temperature are shown in Figure 1. Both spectra display a good mirror image, indicative of a very modest distortion in the excited state; there are slight differences in their epsilon values—higher for **4**—and in the energies of their transition sequences—lower for **4**—compared with those of **3**. The absorption spectrum of the bis-porphyrin tweezers **1** is shown in Figure 2, in which it is compared with the absorption spectrum of the model zinc–porphyrin **2** and the cumulative absorption spectrum of two units of **4** and one unit of **3**, which should represent the contribution of the anthracene components to the absorbance of **1**. From the absorption spectrum of **1** the following conclusions can be derived: 1) the porphyrin chromophores absorb nearly all the light over the whole spectral range except at around 380–390 nm, where the anthracene units absorb about 60% of the light, and 2) the spectrum of array **1** is not a simple superposition of the component units, the main difference involving a broadening of the Soret band of the zinc–porphyrin components, a modest decrease in the absorption coefficients over the Soret and Q bands (note that only the absorption of a single unit of **2** is reported in Figure 2), and the appearance of a new band at around 450 nm. The latter, which has previously been observed in an anthracene-linked zinc–porphyrin,[18] has to be ascribed to a sizeable electronic coupling of the transitions of anthracene and zinc–porphyrin (Soret band), which are of similar energies (see Figures 1 and 2).

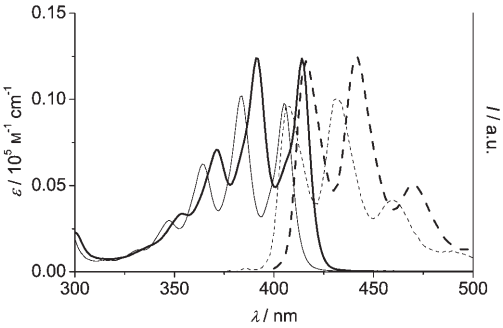

Figure 1. Absorption (continuous lines) and arbitrarily scaled emission spectra (dashed lines) of **3** (thin lines) and **4** (thick lines) in toluene.

The emission spectrum of **1** is very similar to that of the reference porphyrin **2**, with an emission quantum yield that is identical. The fluorescence quantum yield of **1**, excited either at 383 nm, where 60% of the light is absorbed by the anthracene units, or at 551 nm, whereby the light is absorbed only by the zinc–porphyrin component, is the same within experimental error (Table 1). Excitation at 383 nm of a solution of **1** (1×10^{-6} M) is compared in Figure 3 with the excitation of a solution containing the components **3** (1×

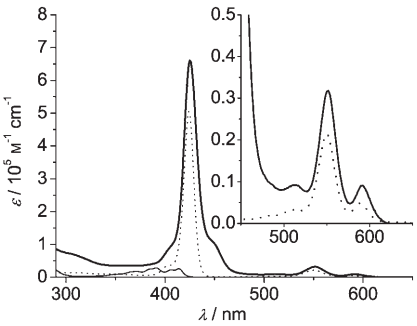

Figure 2. Absorption spectra in toluene of **1** (thick continuous line), **2** (dotted line) and the anthracene components (thin continuous line) obtained by adding the molar absorption coefficients of two units of **4** plus one unit of **3**.

Table 1. Luminescence properties of **1**, the model component units **2**–**4** and the porphyrin guests **5**–**7** in toluene.

	298 K			77 K		
	λ_{max} [nm]	φ_{fl}[a]	τ [ns]	λ_{max} [nm]	τ [ns]	E [eV][b]
1	598	0.08[c] 0.075[d]	2.04	596	3.0	2.07
2	596	0.08	2.3	596	2.6	2.08
3	406	0.87	5.3	408	6.5	3.05
4	416	0.82	4.5	416	5.1	2.98
5[e]	628	0.11	9.7	620	–	2.00
6[e]	648	0.13	9.0	644	–	1.93
7[f]	648	0.11	9.3	640	14.8	1.94

[a] Fluorescence quantum yields, the standards used are anthracene and **2**,[19] see the Experimental Section for details. [b] Derived from the emission maxima at 77 K. [c] Excitation at 551 nm. [d] Excitation at 385 nm. [e] From reference [14e]. [f] From reference [14f].

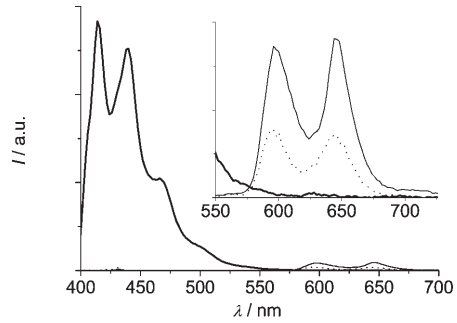

Figure 3. Emission spectra in toluene of solutions of **1** (thin continuous line), **2** (dotted line) and a mixture of **3** and **4** (thick continuous line) excited at 383 nm. The concentrations of the components are 1×10^{-6} M for **1** and **3** and 2×10^{-6} M for **2** and **4**.

10^{-6} M) and **4** (2×10^{-6} M) and a solution of **2** (2×10^{-6} M) and it shows that in **1** the emission due to the anthracene components is totally quenched whereas the emission from the porphyrin component is sensitized relative to the pertinent models. This points to an extremely efficient intramolecular energy transfer from the anthracene units to the zinc–porphyrin chromophores in **1**, as expected on the basis of the good overlap between the emission of **3** and **4** and the absorption band of **2** (Soret region) and on their not exceedingly large mutual distance, about 12 Å for **4** and about 22 Å for unit **3**. The luminescence lifetime for the tweezers **1**, 2.04 ns at 298 K and 3 ns at 77 K, is very similar to that of the zinc–porphyrin model **2**, 2.3 ns at 298 K and 2.6 ns at 77 K, indicating that in spite of some perturbation, the chromophore in the array retains typical porphyrin properties. The components **3** and **4** emit quite strongly, about three times that of unsubstituted anthracene, but their luminescence lifetimes, 5.3 ns for **3** and 4.5 ns for **4** at 298 K, are very similar to that of anthracene in apolar solvents, 5.3 ns.[19a] In **1** the anthracene-based luminescence could not be detected with an apparatus characterized by a 20 ps resolution, indicating an energy-transfer rate constant from the anthracenes to porphyrin higher than 5×10^{10} s^{-1}. This energy transfer could occur in a stepwise fashion from **3** to **4** and finally to the zinc–porphyrin component, but we are unable to resolve such rapid processes. The luminescence data are summarized in Table 1.

Complexation

Zinc–porphyrins are known to bind pyridine or pyridyl residues through an axial bond of the Zn^{II} ion with association constants of the order of 10^4 M^{-1}. These constants have been found to increase by several orders of magnitude when multiple bonds contribute to the formation of the complex and in the presence of a size-matching between host and guest.[4–6,14a–f]

The maximum aperture of the cavity of **1** in the absence of any strain is 15 Å. Of the porphyrins chosen as potential guests, **5** and **6** have interpyridyl nitrogen distances of about 16 Å, whereas **7** has a distance of about 11 Å (Scheme 1). By taking into account two pyridyl N–Zn bonds, **7** fits perfectly within the cavity, whereas **5** and **6**, with an overall size of 20 Å, will not fit inside the cavity unless some distortion in the host occurs.

The free-base dipyridylporphyrins **5**–**7** can clearly approach and axially bind to both zinc–porphyrins of **1** from the outside. Since this is expected to occur with association parameters similar to those displayed by simple pyridine (Pyr), we used this compound as a reference model for external complexation. In contrast, bidentate 4,4′-bipyridine (Bipy), which is known to bind rather strongly in the cavity of **1** in dichloromethane,[5] was identified as a suitable model for internal complexation, that is, the binding of both zinc ions in the same array **1**. Association phenomena between **1** and Pyr or Bipy were therefore examined by spectroscopic techniques.

Complexation with Pyr and Bipy: The absorption and emission changes following the addition of increasing amounts of Pyr to **1** are shown in Figure 4. The association of a pyridyl residue to one zinc–porphyrin moiety (1:1 complex) induces a shift of approximately 6 nm (from 425 to 431 nm) in the Soret band (Figure 4 top) and an even larger change in the

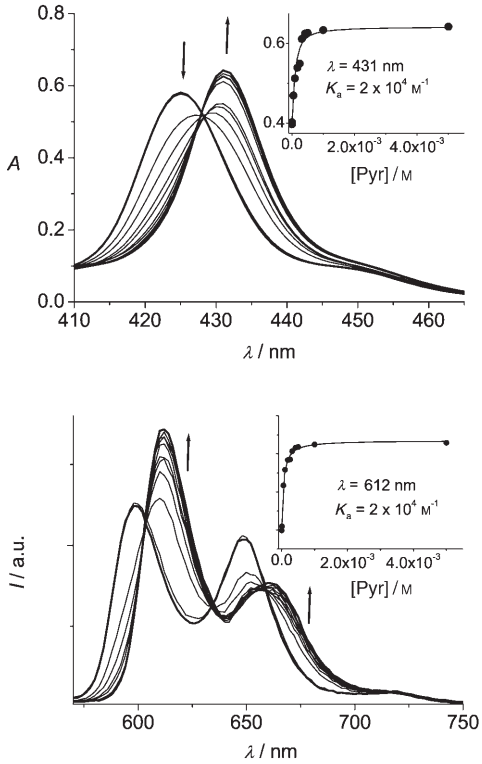

Figure 4. Changes in the absorption and emission of **1** (8.8×10^{-7} M) in toluene solution upon titration with increasing amounts of Pyr (1×10^{-6}–5×10^{-3} M). Top: The change in absorbance of the Soret band region. The fitted data points at 431 nm are shown in the inset. Bottom: The change in emission intensity upon excitation at 428 nm. The fitted data points at 612 nm are shown in the inset.

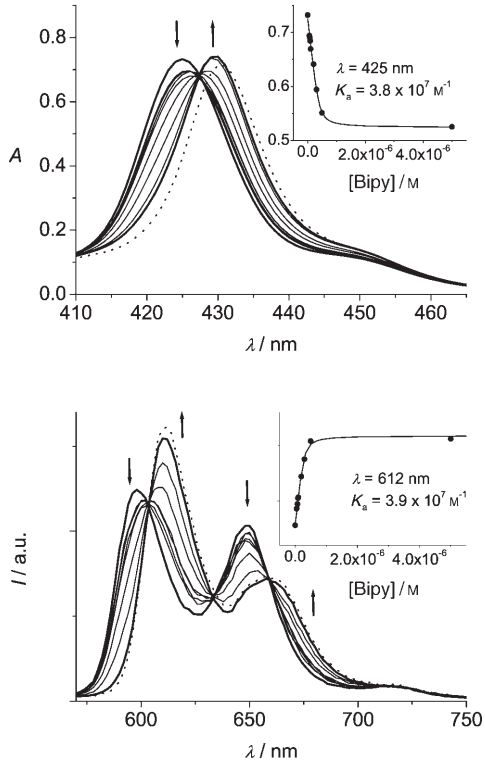

Figure 5. Absorption and emission spectra of compound **1** (1.1×10^{-6} M) in toluene solution upon titration with increasing amounts of Bipy (5×10^{-8}–5×10^{-6} M) are shown as full lines. For further spectral evolution at higher concentrations of Bipy, representing the formation of the 1:1 complex (see text), only the final spectrum for [Bipy] = 5×10^{-3} M is shown as a dotted line. Top: The change in absorbance of the Soret band region. The fitted data points at 425 nm are shown in the inset. Bottom: The change in emission intensity upon excitation at 427.5 nm. The fitted data points at 612 nm are shown in the inset.

emission spectrum of the zinc–porphyrin moiety (Figure 4 bottom) involving a 12 nm bathochromic shift (from 598 to 611 nm and from 648 to 660 nm) of the emission bands and a different intensity distribution in the vibronic progression. Association of one bidentate ligand to two zinc–porphyrins (1:2 complex) induces a smaller bathochromic shift in the absorbance spectrum (from 425 to 429 nm) and an emission spectrum that is essentially identical to that of the 1:1 complex.[20] For a bidentate guest, the formation of a complex with one ligand and one zinc–porphyrin (1:1) is possible and is favored by an excess of guest. Figure 5 shows the absorption and emission spectra of **1** upon addition of increasing amounts of Bipy in a concentration range that favors the formation of a 1:2 complex; further evolution of the spectra with further increases in Bipy concentration corresponds to the formation of the 1:1 complex ($\lambda_{max}=431$ nm) and only the final spectrum at [Bipy] = 5×10^{-3} M is reported. The association constants, $K_a=2\times10^4\,M^{-1}$ for Pyr and $K_a=3.8\times10^7\,M^{-1}$ for Bipy (Table 2), were derived by a nonlinear treatment of the absorption and emission data at the reported wavelength (insets of Figures 4 and 5, Table 2). The data have been analyzed according to a procedure previously developed (see the Experimental Section for details) and the association constants are summarized in Table 2.

Since the nitrogen–nitrogen distance in Bipy is much smaller than the bite of the extended host, approximately 7 Å compared with 15 Å, complexation of Bipy requires a reduction of the bite distance in **1**; this reduction can, in principle, occur by rotation around a single bond to yield a nearly cofacial orientation of the two intermediate anthracene units or by a multiple collapse of the bond angles of the cavity to achieve the required distance. We cannot exclude the possibility that both rearrangements play a role in

Table 2. Association constants K_a [M^{-1}] of **1** and the model **2** in toluene at 298 K as determined by spectrophotometric (Abs) or spectrofluorimetric titration (Em).

	Pyr		Bipy		**5**[a]		**6**[a]		**7**[a]	
	Abs	Em	Abs	Em	Abs	Em	Abs	Em	Abs	Em
1	2.0×10^4	2.0×10^4	3.8×10^7	3.9×10^7	2.0×10^6	1.4×10^6	1.0×10^6	8.0×10^5	4.2×10^6	5.2×10^6
	2.0×10^4[b]		3.8×10^7[b]		1.7×10^6[b]		9×10^5[b]		4.7×10^6[b]	
2	9×10^3[b]	1.2×10^4[b]								

[a] The uncertainty in these determinations is higher than the usual 20% because of the method used for the determination, see text. [b] Average of fluorimetric and photometric determinations.

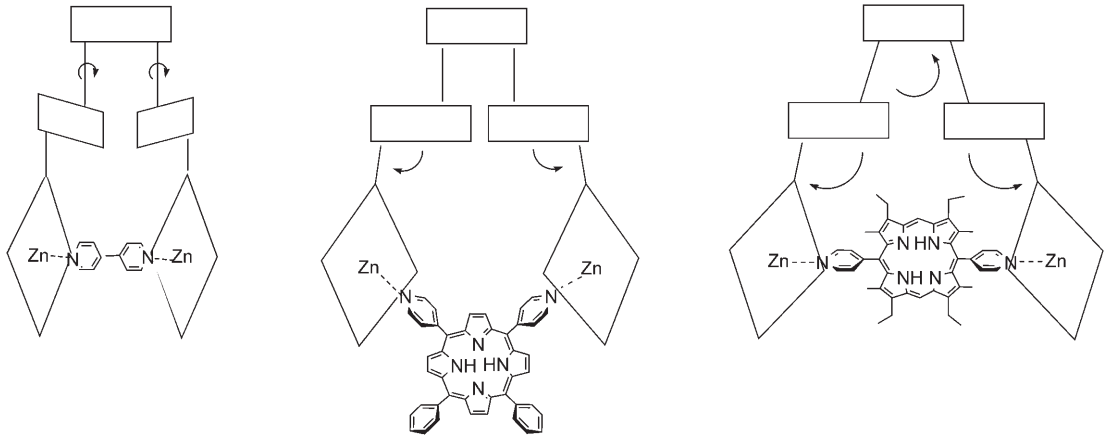

Scheme 3. Different binding modes of tweezers **1**.

adapting the cavity size and orientation to the Bipy guest which is tightly bound (Scheme 3).

Complexation with porphyrins: In order to determine whether the free-base porphyrins **5**–**7** associate with **1**, spectrophotometric and spectrofluorimetric experiments involving the titration of **1** against increasing concentrations of the potential guest were undertaken. This type of experiment is complicated by the fact that the guest strongly absorbs and emits in the same wavelength region as the host (Figure 6 and Table 1). This problem has been addressed in detail previously[21] and, in brief, to analyze the absorption and emission spectra, derived spectral profiles can be used, which can be fitted by the usual equation [see the Experimental Section, Eq. (4)]. The derived spectral profiles, ΔA or ΔI, are obtained by subtraction of the absorption or emission signal of the free-base guest from the experimental signal detected for the mixture of **1** and the guest. Assuming that no spectral changes occur in the free-base porphyrin guest upon complexation, the ΔA profile will represent the changes in the zinc–porphyrin host brought about by complexation and will be comparable, but not necessary identical since in this case the tweezers can have some degree of distortion, to those of Figures 4a and 5a derived for Pyr and Bipy complexation. In contrast, the luminescence of the complex is not only determined by changes brought about by association, as for Pyr and Bipy, but also by the nature of the photoinduced process that can take place in the photoactive components of the complex. In fact, as a consequence of the complexation that brings the partners into close contact, a flux of energy from the singlet excited state of the zinc–porphyrins in **1** (2.07 eV) to the lower-lying singlet excited state (Table 1) of the free-base component **5** (2.0 eV), **6** (1.93 eV), or **7** (1.94 eV) can take place. This will show up as a change in the emission spectrum of the complex **1·*n*** (in which ***n*** represents any free-base porphyrin guest), which will show a decreased contribution from the zinc–porphyrin and an increased contribution from the free-base porphyrin. Owing to the short lifetime of the donor, the photoinduced processes can only take place between partners that are close to each other, that is, in the complex, so the quenching and sensitization phenomena are also strictly correlated to the amount of complex present. Therefore the spectral profile ΔI will contain information both on complexation and on the nature and efficiency of the photoinduced process occurring within the complex.

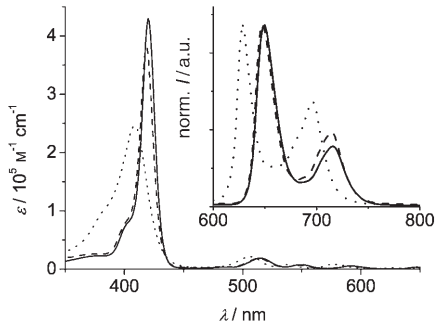

Figure 6. Absorption and emission spectra (inset) in toluene of **5** (dotted line), **6** (continuous line), and **7** (dashed line).

Figure 7 shows ΔA following the addition of increasing amounts of free-base porphyrin **5**, **6**, and **7** respectively, to a constant concentration of **1**. The concentration range explored is limited by the high absorbance of the solutions; in order to avoid the nonlinear instrumental region, measurements were performed with a constant concentration of **1** ($7–8\times10^{-7}$ M) and up to an excess of guest of about 2–2.5 times. The spectral changes of **1** upon interaction with the three free-base porphyrins are similar, and are characterized by a decrease in the Soret band absorbance and a shift of its maximum to lower energies. It is, however, evident that different extents of complexation are achieved in the three cases: **7** > **5** > **6**. Because of the limited concentration range of guest which could be used (see above), the uncertainty of this determination is larger than the usual 20%. The association constants K_a reported in Table 2 were derived by fitting the experimental data (insets of Figure 7).

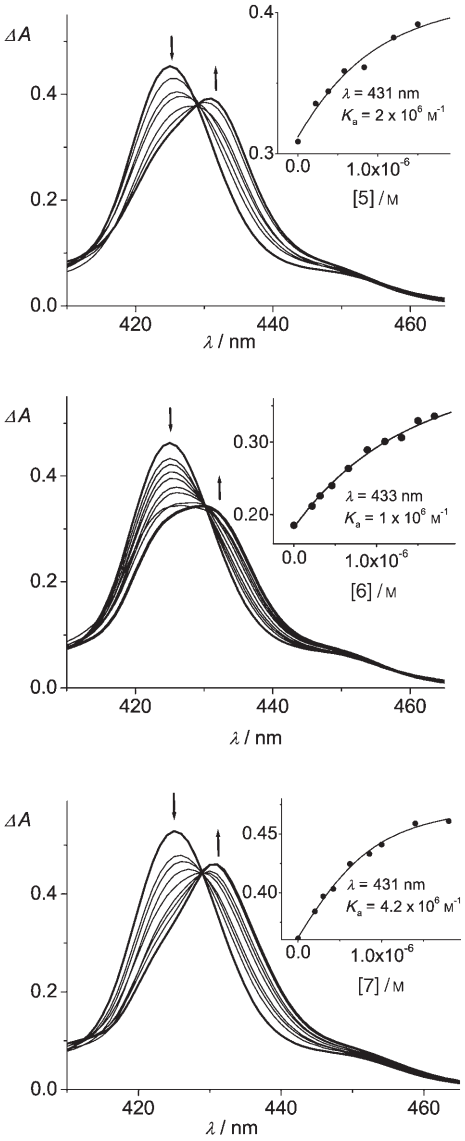

Figure 7. Top: ΔA for compound **1** (6.9×10^{-7} M) in toluene solution upon titration with increasing amounts of **5** (2.2×10^{-7}–1.5×10^{-6} M). The inset displays the fitted experimental points at 431 nm. Middle: ΔA for compound **1** (7×10^{-7} M) in toluene solution upon titration with increasing amounts of **6** (2.2×10^{-7}–1.7×10^{-6} M). The inset shows the fitted experimental points at 433 nm. Bottom: ΔA for compound **1** (8×10^{-7} M) in toluene solution upon titration with increasing amounts of **7** (2×10^{-7}–1.8×10^{-6} M). The inset shows the fitted experimental points at 431 nm.

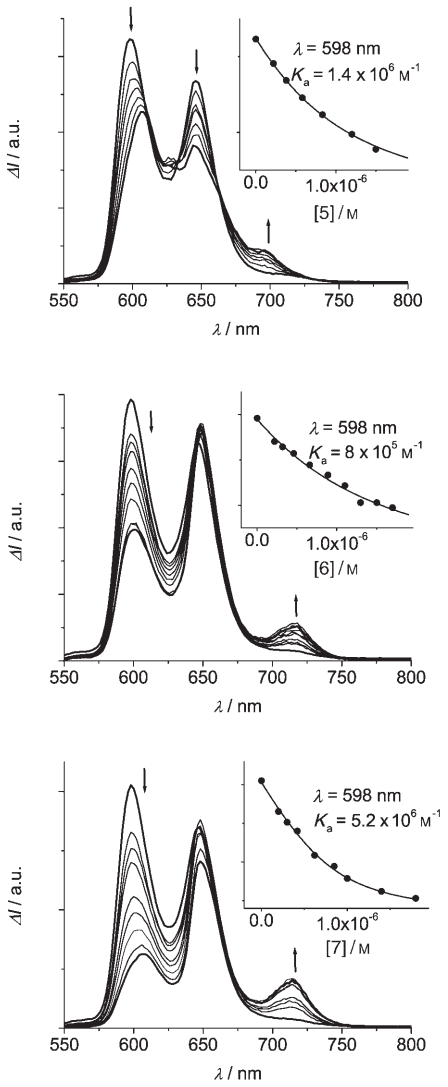

Figure 8. Top: ΔI for excitation at 429 nm of **1** (6.9×10^{-7} M) in toluene solution upon titration with increasing amounts of **5** (2.2×10^{-7}–1.5×10^{-6} M). The inset shows the fitted experimental points at 598 nm. Middle: ΔI for excitation at 430 nm of **1** (7×10^{-7} M) in toluene solution upon titration with increasing amounts of **6** (2.2×10^{-7}– 1.7×10^{-6} M). The inset shows the fitted experimental points at 598 nm. Bottom: ΔI for excitation at 429 nm of **1** (8×10^{-7} M) in toluene solution upon titration with increasing amounts of **7** (2×10^{-7}–1.8×10^{-6} M). The inset displays the fitted experimental points at 598 nm.

The results of fluorimetric titrations upon excitation at the isosbestic points of **1** and the complexes **1·*n*** for the same sets of solutions are shown in Figure 8 as ΔI, after correction for the direct emission of the guests. The nonlinear fittings to experimental data are reported in the insets and the derived association constants are reported in Table 2. The agreement with the values of K_a derived from the absorption titrations is reasonably good in view of the uncertainty associated with these determinations and from the average of the photometric and fluorimetric determinations mean values of 1.7×10^6 M^{-1} for **5**, 9×10^5 M^{-1} for **6**, and 4.7×10^6 M^{-1} for **7** have been calculated.

The association constants of the dipyridyl–porphyrin guests are higher by two orders of magnitude than those of the monodentate Pyr and point to an interaction of the guest with the inside of the cavity rather than with the outside. Guest **7**, which best fits the dimensions of the tweezers, displays the highest association constant, $K_a = 4.7\times10^6$ M^{-1}, which is lower by nearly one order of magnitude than the Bipy case. The fact that **7** can approach the cavity in a non-axial geometry with respect to the zinc ions of **1** could bias the bidentate coordination in spite of the favorable size parameter compared with Bipy (see Scheme 2). It should, in fact, be noted that the association constant of **7** with **1** is

lower by two orders of magnitude than that determined for **7** with an oblique bis-porphyrin host able to give perfect axial geometry coordination in addition to good size-matching.[14f]

For **5** and **6**, as discussed above, a cavity distortion of nearly 5 Å is needed to allow bidentate complexation. Though **1** is rather rigid, a larger aperture of the bite could be achieved by multiple small-angle distortions in the structure of the bis-porphyrin tweezers, which could be affordable with low-energy costs. Recently, force-field calculations have shown that compression and expansion of the side-walls in a molecular clip with anthracene side-walls are low-energy processes.[22] The energy necessary for the expansion can be compensated by the formation of new bonds in the host–guest complex. Very likely, concerted rotation and distortion occur to accommodate large as well as small guests (Scheme 3). However, the distortion needed to accommodate the two *trans*-dipyridylporphyrins can explain the lower association constants of **5** and **6**, of the order of $10^6\,\text{M}^{-1}$, relative to **7**. Also, note that the presence of bulky *tert*-butylphenyl groups in **6** causes the binding to **1** to be weaker than in **1·5** in spite of the same N–N distance. On the other hand the association constants of **5** and **6** are 100 and 50 times higher, respectively, than that of Pyr and so the association cannot be ascribed only to external binding.

To fully exploit other possible association modes responsible for the spectral changes observed, we considered the possibility of π–π stacking of the free-base porphyrin guests with the anthracene or the porphyrin units of **1**. As already pointed out, after rotation around single bonds the two anthracene and porphyrin units can come parallel and rather close (ca. 5 Å) and this could be an ideal site for such an interaction. We reasoned that a simple tetraphenylporphyrin (TPP, Scheme 1) would serve as a model for this type of interaction and determined the spectral changes following the addition of TPP to a solution of **1** in toluene (7.4×10^{-7} M). No effect on the spectral properties of **1** were detected up to a concentration of TPP of 5×10^{-6} M, largely exceeding the concentrations of **5**, **6**, and **7** used. This result rules out the possibility that our guests are involved in this type of interaction in the concentration range explored.

We have therefore confirmed our model of inclusion by the tweezers cavity of all the porphyrin guests, including the larger **5** and **6**, and this implies that the cavity in **1** can open up to approximately 20 Å. This conclusion, together with the previous observation of the ability of the cavity to shrink the bite through rotation around single bonds and so complex small bidentate ligands efficiently, makes **1** an extremely versatile building block for the assembly of porphyrin-based noncovalent architectures. It should be pointed out that whereas several bis(zinc–porphyrin) tweezers have been reported that are able to reduce the bite and bind smaller guests,[3h,14c] this is the first report of this type of tweezers in which the cavity can open very wide, by about 30%, to accommodate larger guests.

Photoinduced processes in the complexes: As discussed above, when **1** is complexed with a photoactive component, luminescence spectra also indicate the occurrence of photoinduced processes. From an inspection of Figure 8 (middle and bottom), it is evident that upon association of **1** with **6** and **7** there is quenching of **1**, as testified by the decrease in the 598 nm band without any spectral shift, and a concomitant sensitization of the free-base porphyrin bands, as shown by the increase in the 700–720 nm emission, which is unique to the free-base guest (see Figure 6). In these cases no luminescence from the complexes, characterized by bands at 612 and 660 nm (see Figures 4b and 5b) could be detected indicating an extremely fast energy transfer. Less straight forward is the interpretation of the results of the **1·5** complex system shown in Figure 8 (top). Upon complexation, a decrease in the emission band at 598 nm and a concomitant shift in the emission to 610 nm can be detected, which is accompanied by an increase in the emission at 696 nm, corresponding to the emission maximum of the guest **5**. Therefore sensitization of the guest is discernible, but at variance with the other cases, the quenching of the emission of **1** at 598 nm is accompanied by a shift to 610 nm. This is interpreted as an increased contribution to the detected emission from the complex form **1·5**, which is expected to display a maximum at 612 nm, similarly to what occurs in the Bipy or Pyr complexes. This implies a reduced efficiency in the quenching of **1** by **5** within the complex compared with the cases of **6** and **7**.

Time-resolved determinations in the pico- and nanosecond range have been performed in order to derive kinetic parameters for the energy-transfer processes. Picosecond excitation at 532 nm was performed on solutions of **1** (1×10^{-5} M) with **5**, **6**, and **7** with a fast-streak camera-detection system. The concentration of guest was approximately 8×10^{-6} M leading to incomplete complexation of **1**, but the use of higher guest concentrations was prevented by solubility problems. The time-resolved decay of the **1** component was determined at 600 nm and the growth in the luminescence of the free-base guests was determined at 715 nm for complexes **1·6** and **1·7** and at 700 nm for complex **1·5**. The results are collected in Figure 9; the decay is fitted by a bi-exponential law for all systems and for both wavelengths. At short reaction times a fast decay followed by an approximate 2 ns lifetime occurs at 600 nm, whereas a fast growth followed by a lifetime of about 9 ns is detected in the 700–720 nm region. The lifetimes of the fast decay at 600 nm and of the growth at around 700–720 nm are in good agreement for each system: 42 ps for **6** and **7** and 120 ps for **5**. This reaction, which is interpreted as an energy-transfer process from **1** to the free-base porphyrin guest, has the following rate constants (calculated as $k_{en}=1/\tau-1/\tau_0$): $7.8\times10^9\,\text{s}^{-1}$ for **5** and $2.3\times10^{10}\,\text{s}^{-1}$ for **6** and **7**. The efficiency is nearly quantitative: 98% for **6** and **7** and 95% for **5**. By comparison with the data in Table 1, the decays of approximately 2 ns at 600 nm and of ca. 9 ns at around 700–720 nm are identified as the luminescence lifetimes of uncomplexed **1** and of the free-base guest units in the complex, respectively.

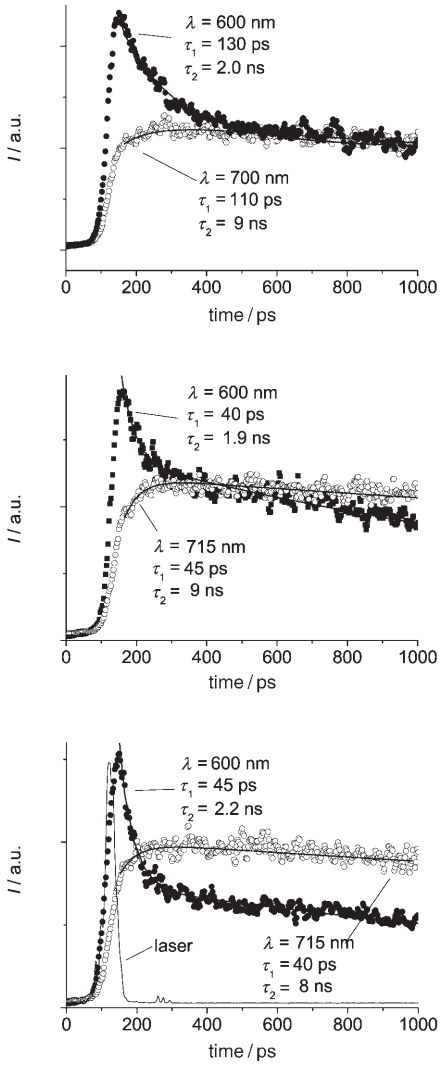

Figure 9. Time-resolved luminescence of **1** (1×10^{-5} M) in toluene solutions upon excitation at 532 nm (35 ps, 1.5 mJ) in the presence of **5** (8×10^{-6} M) (top); **6** (8×10^{-6} M) (middle); and **7** (8×10^{-6} M) (bottom). Decay of the luminescence donor at 600 nm (●) and growth of the free-base acceptor at 715 nm for **6** and **7** and at 700 nm for **5** (○).

An energy-level diagram (Scheme 4) can be drawn from the spectroscopic data of Table 1, and the calculated values of $\Delta G°$ for the energy-transfer process are $\Delta G° = -0.07$ eV for the system **1·5**, $\Delta G° = -0.14$ eV for the system **1·6**, and $\Delta G^0 = -0.13$ eV for the system **1·7**. The lower driving force for energy transfer in complex **1·5** is in agreement with the lower rate constant detected in this system, 7.8×10^9 s^{-1} relative to 2.3×10^{10} s^{-1} for **1·6** and **1·7**.

Energy transfer between singlet states can occur by two different mechanisms, the Förster (or dipole–dipole interaction) and the Dexter (or electron exchange) mechanisms.[23,24] When strongly emitting donors and strongly absorbing acceptors such as porphyrins are involved, the mechanism is generally of the former type. In this case it is possible to calculate, on the basis of geometric, spectroscopic, and photophysical data, the rate constant of the process,

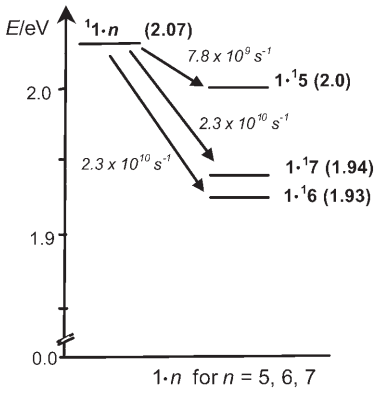

Scheme 4. Energy-level diagram of the complexes **1·*n***, where ***n*** = **5**, **6**, and **7**.

k_{en}^F, by means of Equation (1),[23] in which Φ and τ are the emission quantum yield (0.08) and lifetime (2 ns) of the donor **1**, respectively, d_{DA} is the donor–acceptor center-to-center distance (ca. 10 Å in all cases), n is the refractive index of toluene, and J^F is the overlap integral calculated from the luminescence spectrum of the donor, $F(\bar{\nu})$, and the absorption spectrum of the acceptor, $\varepsilon(\bar{\nu})$ [Eq. (2)].

$$k_{en}^F = \frac{8.8\times10^{-25}\kappa^2\Phi}{n^4\tau d_{DA}{}^6}J^F \quad (1)$$

$$J^F = \frac{\int F(\bar{\nu})\varepsilon(\bar{\nu})/\bar{\nu}^4 d\bar{\nu}}{\int F(\bar{\nu})d\bar{\nu}} \quad (2)$$

The calculated value of J^F is 2.34×10^{-14} cm^3 M^{-1} when **5** is the acceptor, 3.54×10^{-14} cm^3 M^{-1} when **6** is used, and 3.37×10^{-14} cm^3 M^{-1} when **7** is the acceptor. The parameter κ^2 in Equation (1) is the orientation factor and takes into account the relative orientation of the transition dipole moments of the donor and the acceptor. Whereas the value is statistical ($^2/_3$), in a couple of reacting partners that freely diffuse in solution, since they are randomly approaching, the value for κ^2 can be quite different when the two partners are locked in rigid positions with respect to each other. In this case κ^2 can be calculated from Equation (3),[25] in which θ_D and θ_A are the angles formed between the line connecting the donor and acceptor centers and the transition moments of the donor and acceptor, respectively, and ϕ is the angle between the projections of the transition moments on a plane perpendicular to the line connecting the centers of the donor and acceptor.

$$\kappa^2 = (\sin\theta_D\sin\theta_A\cos\phi - 2\cos\theta_D\cos\theta_A)^2 \quad (3)$$

The transition dipole of the zinc–porphyrin donor is degenerate in the plane of the tetrapyrrolic rings and the transition dipole of the free-base porphyrin guests is oriented along the direction of the pyrrolic nitrogen atom.[26] If we assume that in the formation of the complex a nearly axial coordination is maintained, $\theta_D = 90°$ and $\theta_A = 45°$ for **5**, **6**,

and **7**, whereas ϕ varies between 0 and 360°. Under these conditions the average value of κ^2 is of the order of 0.2 for all systems. By introducing this value together with the other parameters into Equation (2), rate constants of $k_{en} \sim 3\times10^{10}$ for **1·5** and $k_{en} \sim 4\times10^{10}$ for **1·6** and **1·7** are derived. In view of the many simplifications introduced into these calculations and of the several limits of this theory in describing closely spaced large chromophores as in the present case,[27] the results can be considered to be in acceptable agreement with the experimental results, $7.8\times10^{9}\ s^{-1}$ for **1·5** and $2.3\times10^{10}\ s^{-1}$ for **1·6** and **1·7**, since they reproduce both the order of magnitude and the relative reactivity scale. This suggests that a Förster-type energy-transfer mechanism is operative within the complexes formed by **1** and the free-base dipyridylporphyrin guests.

Conclusions

We have synthesized and photophysically characterized the bis(Zn^{II}–porphyrin) tweezers **1** with anthracene components as apex and side-arms. These tweezers can bind pyridyl residues through axial coordination to the zinc ions of porphyrins and we have shown that **1** has excellent binding properties with bidentate pyridyl guests of very different dimensions. In fact it binds to 4,4′-bipyridine (ca. 7 Å), *cis*-dipyridylporphyrin free-base (ca. 11 Å), and *trans*-dipyridylporphyrin free-base (ca. 16 Å) with association constants $>9\times10^{5}\ M^{-1}$. This is made possible by the ability of the cavity to adjust its bite: rotation through single bonds can reduce the size of the cavity whereas multiple slight distortions of the angles in the scaffold can open or close the bite in order to accommodate guests of different sizes. Very likely, concerted rotation and distortion occur to bind guests of very different sizes with remarkably high association constants. Photoinduced energy transfer in the triporphyrin complexes from the host to the guest is nearly quantitative and the results are compatible with a dipole–dipole mechanism with a reduced orientation factor.

Experimental Section

Spectroscopic and photophysical determination: NMR spectra were recorded on a Bruker AC 300 (300 MHz) or a Bruker ARX500 (500 MHz) with solvent peaks as reference. FAB mass spectra in positivemode were acquired on an Autospec (VG). Spectroscopic grade toluene was used (C. Erba). Pyridine (Aldrich) and 4,4′-bipyridine (Merck) were used as received. Absorption spectra were recorded with a Perkin-Elmer Lambda 9 spectrophotometer and emission spectra, uncorrected if not otherwise specified, with a Spex Fluorolog II spectrofluorimeter equipped with a Hamamatsu R928 photomultiplier. Relative luminescence intensities were evaluated from the area (on an energy scale) of the luminescence spectra corrected for the photomultiplier response. Luminescence quantum yields for anthracene derivatives were obtained by reference to anthracene in toluene ($\varphi_{fl}=0.3$).[19a] For the porphyrin components, the emission quantum yields were obtained by reference to (5,10,15,20-tetra-*tert*-butylphenyl)porphyrinatozinc(II) in toluene ($\varphi_{fl}=0.08$).[19b] Experiments at 77 K were performed by using quartz capillary tubes immersed in liquid nitrogen contained in a home-made quartz Dewar flask.

Titration experiments for the determination of the association constants were performed by using a constant concentration of **1**, in the range of 7×10^{-7}–1.1×10^{-6} M, and variable concentrations of Pyr, Bipy, **5**, **6**, and **7**. In the titration experiments excitation was performed at the isosbestic point of the complexed and uncomplexed zinc–porphyrin spectra. Equation (4) was used to determine the association constant K_a, whereby $K_a = 1/K_d$. Obs is any observable (i.e., absorbance or emission intensity or ΔA and ΔI, as detailed in the text), S_0 is the constant concentration of **1**, X is the variable concentration of the complexing agent, ΔObs is the maximum variation of the observable under examination, and Obs_0 is its value at zero concentration of titrating agent.[21,28]

$$Obs = Obs_0 + \frac{\Delta Obs}{2S_0}\{K_d + X + S_0 - [(K_d + X + S_0)^2 - 4XS_0]^{1/2}\} \quad (4)$$

Fluorescence lifetimes in the nanosecond range were detected by using an IBH time-correlated single-photon-counting apparatus with excitation at 337 nm. Luminescence lifetimes in the picosecond range were determined with an apparatus based on a Nd:YAG laser (Continuum PY62-10) with a 35 ps pulse duration (1.5 mJ pulse^{-1}) at 532 nm, and a fast-streak camera-detection system (Hamamtsu C1587 equipped with M1952). The luminescence signals from 1000 laser shots were averaged and the time profile was measured from the streak image in a wavelength range of about 20 nm around the selected wavelength. The luminescence decays were fitted by using standard iterative nonlinear programs, taking into consideration the instrumental response.[29]

Computation of the integral overlap and of the rate of energy transfer according to the Förster mechanism were performed with the use of Matlab 5.2.[30]

Molecular dimensions and distances were estimated by using CS Chem 3D Ultra 6.0 software.[31]

Estimated errors are 10% on lifetimes, 20% on quantum yields, and 20% on association constants, except for the equilibria involving two porphyrins for which uncertainties are of the order of 30–40%. Working temperatures, if not otherwise specified, are 295 ± 2 K.

1,5-Bis(triethylsilylethynyl)anthracene (4): Triethylsilylacetylene (3.1 mL, 17.5 mmol) and a 1 M solution of ethylmagnesium bromide in THF (17.5 mmol, 17.5 mL) were added to distilled THF (6.5 mL). The solution was stirred for 45 min at 0 °C under argon. The mixture was then added to a solution of 1,5-dichloroanthracene (864 mg, 3.5 mmol, 1 equiv), Ni(acac)$_2$ (1.8 mg, 6.57 mmol, 2 equiv), and PPh_3 (3.8 mg, 10.9 mmol, 3 equiv) in distilled THF (39 mL). Whilst stirring, the solution was refluxed for 3 days under argon. After column chromatography, the desired product **4** was isolated in 25% yield (398 mg, 0.87 mmol) as a yellow solid. ^{1}H NMR (300 MHz, $CDCl_3$): $\delta = 8.94$ (s, 2H; 9,10-H), 8.02 (dd, $^3J = 8.4$, $^4J = 0.9$ Hz, 2H; 4,8-H), 7.75 (dd, $^3J = 6.9$, $^4J = 1.1$ Hz, 2H; 2,6-H), 7.43 (dd, $^3J = 8.6$, $^3J = 7.0$ Hz, 2H; 3,7-H), 1.18 (t, $^3J = 8.2$ Hz, 18H; -CH_3 (TES)), 0.81 ppm (q, $^3J = 7.9$ Hz, 12H; -CH_2 (TES)).

1-Ethynyl-5-triethylsilylethynylanthracene (8): Compound **4** (250 mg, 0.55 mmol, 1 equiv) was dissolved in a 85:15 mixture of THF/MeOH (8 mL). K_2CO_3 was added (562 mg, 4.39 mmol, 8 equiv). The reaction mixture was stirred for 6 h 30 min. The resulting suspension was filtered through a glass frit and the solvent was evaporated. The crude product was dissolved in dichloromethane and the resulting organic phase washed with a saturated NH_4Cl solution and distilled water. After column chromatography, the desired product **8** was obtained in 43% yield (80 mg, 0.23 mmol) as a yellow solid. ^{1}H NMR (300 MHz, $CDCl_3$): $\delta = 8.96$ (s, 1H; 9- or 10-H), 8.91 (s, 1H; 9- or 10-H), 8.06 (dd, $^3J = 8.1$, $^4J = 0.6$ Hz, 2H; 4,8-H), 7.77 (dd, $^3J = 6.6$, $^4J = 1.1$ Hz, 2H; 2,6-H), 7.45 (dd, $^3J = 8.6$, $^3J = 6.9$ Hz, 1H; 3- or 7-H), 7.44 (dd, $^3J = 8.6$, $^3J = 7.0$ Hz, 1H; 3- or 7-H), 3.59 (s, 1H; $H_{acetylene}$), 1.17 (t, $^3J = 7.9$ Hz, 9H; -CH_3 (TES)), 0.81 ppm (q, $^3J = 7.5$ Hz, 6H; -CH_2 (TES)).

Porphyrin/anthracene conjugate 10: Compound **8** (100 mg, 0.29 mmol, 1 equiv) and 5-(*p*-iodophenyl)-10,15,20-tris(3,5-*tert*-butylphenyl)porphyrinatozinc(II) (334 mg, 0.29 mmol, 1 equiv) were dissolved in degassed

NEt_3 (24 mL). $[Pd_2(PPh_3)_2Cl_2]$ (5.5 mg, 7.3 μmol, 0.025 equiv) and CuI (3 mg, 14.6 μmol, 0.05 equiv) were added. The reaction mixture was stirred overnight under argon at room temperature. The solvent was evaporated and the crude product dissolved in dichloromethane. The resulting organic phase was washed with a 0.35 M solution of $Na_2S_2O_3$, a 2% solution of disodium EDTA, a saturated solution of NH_4Cl and distilled water. After column chromatography, the desired compound **10** was isolated in 58% yield (228 mg, 0.17 mmol) as a violet, glassy product. ^{1}H NMR (300 MHz, $CDCl_3$): $\delta = 9.19$ (s, 1H; 9- or 10-H), 9.05 (d, $^3J = 4.6$ Hz, 2H; β-H), 9.03 (d, $^3J = 4.6$ Hz, 2H; β-H), 9.02 (s, 4H; β-H), 9.02 (s, 1H; 9- or 10-H), 8.33 (d, $^3J = 8.4$ Hz, 2H; *o*-H), 8.21 (d, $^3J = 6.9$ Hz, 1H; 4-H), 8.13 (d, $^3J = 4.6$ Hz, 1H; 8-H), 8.13 (d, $^3J = 8.4$ Hz, 2H; *m*-H), 8.11 (d, $^4J = 1.8$ Hz, 4H; *o*′-H), 8.10 (d, $^4J = 1.4$ Hz, 2H; *o*″-H), 7.97 (dd, $^3J = 6.9$, $^4J = 0.9$ Hz, 1H; 2-H), 7.80 (t, $^4J = 1.5$ Hz, 3H; *p*′-, *p*″-H), 7.80 (d, $^3J = 3.7$ Hz, 1H; 6-H), 7.58 (dd, $^3J = 8.6$, $^3J = 7.0$ Hz, 1H; 3- or 7-H), 7.49 (dd, $^3J = 8.6$, $^3J = 7.0$ Hz, 1H; 3- or 7-H), 1.54 (s, 36H; *t*Bu), 1.53 (s, 18H; *t*Bu), 1.17 (t, $^3J = 7.7$ Hz, 9H , CH_3 (TES)), 0.81 ppm (q, $^3J = 7.6$ Hz, 6H; CH_2 (TES)); UV/Vis (CH_2Cl_2): λ_{max} (ε) = 425 (497000), 552 (19700), 593 nm (7900 $M^{-1}cm^{-1}$).

Porphyrin/anthracene conjugate 11: Porphyrin/anthracene conjugate **10** (220 mg, 0.16 mmol, 1 equiv) was dissolved in a 50:50 mixture of THF/MeOH (6 mL). Potassium carbonate (166 mg, 1.30 mmol, 8 equiv) was added and the reaction mixture was stirred for 6 h under argon. The suspension was filtered through a glass frit and the solvent was evaporated. The crude product was dissolved in dichloromethane and the resulting organic phase was washed with a saturated solution of NH_4Cl and distilled water. After column chromatography, the desired product was isolated in 87% yield (175 mg, 0.14 mmol). as a violet, glassy product. ^{1}H NMR (300 MHz, $CDCl_3$): $\delta = 9.20$ (s,1H; 9- or 10-H), 9.05 (d, $^3J = 4.6$ Hz, 2H; β-H), 9.03 (d, $^3J = 4.6$ Hz, 2H; β-H), 9.02 (s, 4H; β-H), 9.02 (s, 1H; 9- or 10-H), 8.33 (d, $^3J = 6.5$ Hz, 2H; *o*-H), 8.24 (d, $^3J = 8.8$ Hz, 1H; 4-H), 8.17 (d, $^3J = 8.8$ Hz, 1H; 8-H), 8.17 (d, $^3J = 6.4$ Hz, 2H; *m*-H), 8.14 (d, $^4J = 1.8$ Hz, 4H; *o*′-H), 8.11 (d, $^3J = 1.7$ Hz, 2H; *o*″-H), 7.97 (dd, $^3J = 6.9$, $^4J = 0.9$ Hz, 1H; 2-H), 7.80 (t, $^4J = 1.5$ Hz, 3H; *p*′-, *p*″-H), 7.80 (d, $^3J = 3.7$ Hz, 1H; 6-H), 7.58 (dd, $^3J = 8.5$, $^3J = 6.8$ Hz, 1H; 3- or 7-H), 7.51 (dd, $^3J = 8.6$, $^3J = 7.0$ Hz, 1H; 3- or 7-H), 3.60 (s, 1H; $H_{acetylene}$), 1.54 (s, 36H; *t*Bu), 1.53 ppm (s, 18H; *t*Bu); UV/Vis (CH_2Cl_2): λ_{max} (ε) = 425 (429000), 552 (22300), 593 nm (8500 $M^{-1}cm^{-1}$).

1,8-Bis(bromoethynyl)anthracene (12): Compound **3** (150 mg, 0.66 mmol, 1 equiv) was dissolved in acetone (7 mL). *N*-Bromosuccinimide (282 mg, 1.58 mmol, 2.4 equiv) and silver nitrate (13.5 mg, 79.4 μmol, 0.12 equiv) were added and the solution was stirred for 4 h. After evaporation of the solvent, the yellow solid obtained was dissolved in dichloromethane and the organic phase was washed with a 0.35 M solution of $Na_2S_2O_3$ and distilled water. After purification by column chromatography (eluent: hexane/CH_2Cl_2 90:10), the desired compound **12** was isolated in 87% yield (222 mg, 0.58 mmol) as a yellow solid. ^{1}H NMR (300 MHz, $CDCl_3$): $\delta = 9.30$ (s, 1H; 10-H), 8.44 (s, 1H; 9-H), 8.02 (dd, $^3J = 8.6$, $^4J = 0.6$ Hz, 2H; 4,5-H), 7.72 (dd, $^3J = 7.0$, $^4J = 1.0$ Hz, 2H; 2,7-H), 7.43 ppm (dd, $^3J = 8.6$, $^3J = 7.0$ Hz, 2H; 3,6-H).

Tweezers 1: Porphyrin/anthracene conjugate **11** (70 mg, 56.5 μmol, 2 equiv) and compound **12** (11 mg, 28.3 μmol, 1 equiv) were dissolved in degassed DMSO (1 mL). $[Pd_2(dba)_3]$ (1.55 mg, 1.69 μmol, 0.03 equiv), LiI (1.5 mg, 11.3 μmol, 0.2 equiv), CuI (0.27 mg, 1.41 μmol, 0.025 equiv), and 1,2,2,6,6-pentamethylpiperidine (PMP) (30 μL, 0.16 mmol, 2.8 equiv) were added. The reaction mixture was stirred under argon at room temperature for 3 days. Dichloromethane and distilled water were added. The resulting organic phase was washed with a 0.35 M solution of $Na_2S_2O_3$, a 2% solution of disodium EDTA, and distilled water. After preparative chromatography on Al_2O3, the desired tweezers **1** were isolated in 33% yield (25 mg, 9.25 μmol) as a violet, glassy product. ^{1}H NMR (300 MHz, $CDCl_3$): $\delta = 9.78$ (s, 1H; 10-H), 8.93 (d, $^3J = 4.7$ Hz, 4H; β-H), 8.91 (d, $^3J = 4.8$ Hz, 4H; β-H), 8.89 (d, $^3J = 4.4$ Hz, 4H; β-H), 8.88 (d, $^3J = 4.6$ Hz, 4H; β-H), 8.81 (s, 2H; 9′-H), 8.80 (s, 2H; 10′-H), 8.57 (s, 1H; 9-H), 8.25 (d, $^3J = 8.2$ Hz, 4H; *o*-H), 8.13 (d, $^3J = 8.4$ Hz, 4H; *m*-H), 8.13 (d, 2H; 4′-H, hidden), 8.13 (d, 2H; 8′-H, hidden), 7.99 (d, $^4J = 1.7$ Hz, 4H; *o*″-H), 7.98 (d, $^3J = 7.2$ Hz, 2H; 6′-H), 7.92 (d, $^4J = 1.4$ Hz, 8H; *o*′-H), 7.91 (d, 2H; 2′-H, hidden), 7.88 (d, $^3J = 4.2$ Hz, 2H; 4-H), 7.75 (t, $^4J = 1.7$ Hz, 2H; *p*″-H), 7.63 (t, $^4J = 1.8$ Hz, 4H; *p*′-H), 7.57 (dd, $^3J = 8.5$, $^3J = 7.0$ Hz, 2H; 7′-H), 7.49 (dd, $^3J = 8.6$, $^3J = 7.0$ Hz, 2H; 3′-H), 7.26 (d, 2H; 2-H, hidden), 6.95 (dd, $^3J = 8.5$, $^3J = 7.0$ Hz, 2H; 3-H), 1.53 (s, 72H; *t*Bu), 1.48 ppm (s, 36H; *t*Bu); UV/Vis (toluene): λ_{max} (ε) = 425 (661000), 551 (31700), 592 nm (9100 $M^{-1}cm^{-1}$). MS (FAB^+): *m*/*z* calcd for $[M]^+$: 2700.3; found: 2700.3.

Acknowledgements

Financial support from the Italian CNR (Project PM-P04-ISTM-C1: Molecular, supramolecular and macromolecular components with photonic and optoelectronic properties), from COST D31/0003/04, the Ministero dell'Istruzione, dell'Università e della Ricerca (FIRB, RBNE019H9K), as well as from the CNRS and the French Ministry of Research (ACI Jeunes Chercheurs) are gratefully acknowledged. We thank Elisabetta Iengo for a loan of TPP and Vincent Troiani for kindly providing us with porphyrin **5**.

[1] a) O. Shoji, S. Okada, A. Satake, Y. Kobuke, *J. Am. Chem. Soc.* **2005**, *127*, 2201–2210; b) R. Takahashi, Y. Kobuke, *J. Am. Chem. Soc.* **2003**, *125*, 2372–2373; c) Y. Kuroda, K. Sugou, K. Sasaki, *J. Am. Chem. Soc.* **2000**, *122*, 7833–7834; d) R. A. Haycock, A. Yartsev, U. Michelsen, V. Sundström, C. A. Hunter, *Angew. Chem.* **2000**, *112*, 3762–3765; *Angew. Chem. Int. Ed.* **2000**, *39*, 3616–3619; e) T. Hayashi, H. Ogoshi, *Chem. Soc. Rev.* **1997**, *26*, 355–364.

[2] a) H. L. Anderson, *Chem. Commun.* **1999**, 2323–2330; b) C. M. Drain, J. T. Hupp, K. S. Suslick, M. R. Wasielewski, X. Chen, *J. Porphyrins Phthalocyanines* **2002**, *6*, 243–258.

[3] a) I. P. Danks, I. O. Sutherland, C. H. Yap, *J. Chem. Soc. Perkin Trans. 1* **1990**, 421–422; b) H. L. Anderson, C. A. Hunter, M. N. Meah, J. K. M. Sanders, *J. Am. Chem. Soc.* **1990**, *112*, 5780–5789; c) H. L. Anderson, J. K. M. Sanders, *Angew. Chem.* **1990**, *102*, 1478–1480; *Angew. Chem. Int. Ed. Engl.* **1990**, *29*, 1400–1403; d) C. A. Hunter, C. M. R. Low, M. J. Packer, S. E. Spey, J. G. Vinter, M. O. Vysotsky, C. Zonta, *Angew. Chem.* **2001**, *113*, 2750–2754; *Angew. Chem. Int. Ed.* **2001**, *40*, 2678–2682; e) K. Ogawa, Y. Kobuke, *Angew. Chem.* **2000**, *112*, 4236–4239; *Angew. Chem. Int. Ed.* **2000**, *39*, 4070–4073; f) P. N. Taylor, H. L. Anderson, *J. Am. Chem. Soc.* **1999**, *121*, 11538–11545; g) R. V. Slone, J. T. Hupp, *Inorg. Chem.* **1997**, *36*, 5422–5423; h) M. R. Johnston, M. J. Gunter, R. N. Warrener, *Chem. Commun.* **1998**, 2739–2740; i) D. Jokic, C. Boudon, G. Pognon, M. Bonin, K. J. Schenk, M. Gross, J. Weiss, *Chem. Eur. J.* **2005**, *11*, 4199–4209.

[4] J. Brettar, J.-P. Gisselbrecht, M. Gross, N. Solladié, *Chem. Commun.* **2001**, 733–734.

[5] R. Rein, M. Gross, N. Solladié, *Chem. Commun.* **2004**, 1992–1993.

[6] A. Satake, Y. Kobuke, *Tetrahedron* **2005**, *61*, 13–41, and references therein.

[7] a) E. Alessio, M. Macchi, S. Heath, L. G. Marzilli, *Chem. Commun.* **1996**, *12*, 1411–1412; b) C. C. Mak, N. Bampos, S. L. Darling, M. Montalti, L. Prodi, J. K. M. Sanders, *J. Org. Chem.* **2001**, *66*, 4476–4486; c) A. Prodi, C. Chiorboli, F. Scandola, E. Iengo, E. Alessio, R. Dobrawa, F. Würthner, *J. Am. Chem. Soc.* **2005**, *127*, 1454–1462.

[8] U. Michelsen, C. A. Hunter, *Angew. Chem.* **2000**, *112*, 780–783; *Angew. Chem. Int. Ed.* **2000**, *39*, 764–767.

[9] J. E. Redman, N. Feeder, S. J. Teat, J. K. M. Sanders, *Inorg. Chem.* **2001**, *40*, 2486–2499.

[10] a) B. G. Maya, N. Bampos, A. A. Kumar, N. Feeder, J. K. M. Sanders, *New J. Chem.* **2001**, *25*, 797–800; b) L. Giribabu, A. A. Kumar, V. Neeraja, B. G. Maiya, *Angew. Chem.* **2001**, *113*, 3733–3736; *Angew. Chem. Int. Ed.* **2001**, *40*, 3621–3624.

[11] a) H. Yamaguchi, M. Kamachi, A. Harada, *Angew. Chem.* **2000**, *112*, 3987–3989; *Angew. Chem. Int. Ed.* **2000**, *39*, 3829–3831; b) D. R. Reddy, B. G. Maiya, *J. Phys. Chem. A* **2003**, *107*, 6326–6333.

[12] P. P. Kumar, B. G. Maiya, *New J. Chem.* **2003**, *27*, 619–625.

[13] a) V. V. Borokov, G. A. Hembury, Y. Inoue, *Acc. Chem. Res.* **2004**, *37*, 449–459; b) X. Huang, B. Borhan, B. H. Rickman, K. Nakanishi, N. Berova, *Chem. Eur. J.* **2000**, *6*, 216–224; c) R. Paolesse, D. Monti, E. Venanzi, A. Froiio, S. Nardis, C. Di Natale, C. E. Martinelli, A. D'Amico, *Chem. Eur. J.* **2002**, *8*, 2476–2483; d) M. J. Crossley, L. G. Mackay, C. A. Try, *J. Chem. Soc. Chem. Commun.* **1995**, 1925–1927; e) M. Takeuchi, T. Imada, S. Shinkai, *J. Am. Chem. Soc.* **1996**, *118*, 10658–10659; f) M. Harmata, *Acc. Chem. Res.* **2004**, *37*, 862–873.
[14] a) H. Imahori, E. Yoshizawa, K. Yamada, K. Hagiwara, T. Okada, Y. Sakata, *J. Chem. Soc. Chem. Commun.* **1995**, 1133–1134; b) K. Yamada, H. Imahori, E. Yoshizawa, D. Goztola, M. R. Wasielewski, Y. Sakata, *Chem. Lett.* **1999**, 235–236; c) L. Flamigni, M. R. Johnston, L. Giribabu, *Chem. Eur. J.* **2002**, *8*, 3938–3947; d) L. Flamigni, M. R. Johnston, *New J. Chem.* **2001**, *25*, 1368–1370; e) L. Flamigni, A. M. Talarico, F. Barigelletti, M. R. Johnston, *Photochem. Photobiol. Sci.* **2002**, *1*, 190–197; f) E. Iengo, E. Zangrando, E. Alessio, J.-C. Chambron, V. Heitz, L. Flamigni, J.-P. Sauvage, *Chem. Eur. J.* **2003**, *9*, 5879–5887; g) D. Sun, F. S. Tham, C. A. Reed, L. Chacker, M. Burgess, P. D. W. Boyd, *J. Am. Chem. Soc.* **2000**, *122*, 10704–10705; h) M. Dudiè, P. Lhoták, I. Stibor, H. Petøíèková, K. Lang, *New J. Chem.* **2004**, *28*, 85–90; i) H. Iwamoto, M. Yamaguchi, S. Hiura, Y. Fukazawa, *Heterocycles* **2004**, *63*, 2005–2011.
[15] H. E. Katz, *J. Org. Chem.* **1989**, *54*, 2179–2183.
[16] N. Solladié, M. Gross, *Tetrahedron Lett.* **1999**, *40*, 3359–3362.
[17] C. Cai, A. Vasella, *Helv. Chim. Acta* **1995**, *78*, 2053–2064.
[18] K. Kilså, J. Kajanus, J. Mårtensson, B. Albinsson, *J. Phys. Chem. B* **1999**, *103*, 7329–7339.
[19] a) S. L. Murov, I. Carmichael, G. L. Hugh in *Handbook of Photochemistry*, Dekker, New York, **1993**, p. 7; b) M. Dixon, J.-P. Collin, J.-P. Sauvage, L. Flamigni, *Inorg. Chem.* **2001**, *40*, 5507–5517.
[20] a) C. C. Mak, N. Bampos, J. K. M. Sanders, *Angew. Chem.* **1998**, *110*, 3169–3172; *Angew. Chem. Int. Ed.* **1998**, *37*, 3020–3023; b) L. Baldini, P. Ballester, A. Casnati, R. M. Gomila, C. A. Hunter, F. Sansone, R. Ungaro, *J. Am. Chem. Soc.* **2003**, *125*, 14181–14189; c) P. Ballestrer, A. Costa, A. M. Castilla, P. M. Deyà, A. Frontera, R. M. Gomila, C. H. Hunter, *Chem. Eur. J.* **2005**, *11*, 2196–2206.
[21] L. Flamigni, A. M. Malarico, B. Ventura, *J. Porphyrins Phthalocyanines* **2003**, *7*, 317–326.
[22] F.-G. Klärner, B. Kahlert, R. Boese, D. Blaser, A. Juris, F. Marchioni, *Chem. Eur. J.* **2005**, *11*, 3363–3374.
[23] Th. Förster, *Discuss. Faraday Soc.* **1959**, *27*, 7–17.
[24] D. L. Dexter, *J. Chem. Phys.* **1953**, *21*, 836–850.
[25] W. Van Der Meer, G. Coker, S. Y. S. Chen in *Resonance Energy Transfer Theory and Data*, VCH, Weinehim, **1994**, pp. 55–83.
[26] See, for example, reference [18], and references therein.
[27] K. F. Wong, B. Bagchi, P. J. Rossky, *J. Phys. Chem. A* **2004**, *108*, 5752–5763, and references therein.
[28] L. Flamigni, A. M. Talarico, F. Barigelletti, M. R. Johnston, *Photochem. Photobiol. Sci.* **2002**, *1*, 190–197.
[29] L. Flamigni, *J. Phys. Chem.* **1993**, *97*, 9566–9572.
[30] Matlab 5.2, The MathWorks Inc., Natik MA 01760 (USA).
[31] CambridgeSoft.Com, Cambridge Park Drive 100, Cambridge, MA 02140 (USA).

Received: July 8, 2005
Published online: October 13, 2005

